

# DESIGN AND MAGNETIC MEASUREMENTS OF THE FERMILAB MAIN INJECTOR LAMBERTSON

D.E. Johnson, J.E. DiMarco, D.J. Harding, P.S. Martin, J.-F. Ostiguy, D.G.C. Walbridge, R. Baiod\*  
Fermi National Accelerator Laboratory†, P.O. Box 500, Batavia, IL 60510

## Abstract

A new 1.1 Tesla Lambertson for Main Injector injection/extraction and Tevatron injection has been designed and the magnetic properties of the first production magnet have been measured. The Main Injector Lambertsons will be used for injection of 8.9 GeV/c antiprotons from the Antiproton Source and 150 GeV/c antiprotons recycled from the Tevatron, and the extraction of 120 GeV/c protons for antiproton production, 150 GeV/c protons for Tevatron Injection, 120 GeV/c resonant extraction, and the Main Injector abort. This magnet must accommodate Main Injector and Tevatron circulating beam in its field free region while the field region is at all excitation levels with minimal impact on the circulating beam. The design specifications and results of magnetic measurements in both the field region and field free region for the first production magnet are discussed.

## 1 MAGNET GEOMETRY AND MAGNETIC REQUIREMENTS

The Lambertson has a  $\pm 8$  inch field region with a 2 inch gap. The field free region is 2.5 inches wide with a 78 degree opening. The septa thickness is 0.157 inch and has a 0.2 inch radius. The magnet is composed of 4 quarter cores: 2 inner cores (which are encased in a stainless steel vacuum skin, one with a field free region and the other without) and 2 outer cores which make up the return yoke. The inner core assembly extends approximately 4.3 inches beyond the outer core. The last 4.3 inches of the inner quarter core without the field free region is made with non magnetic material (stainless steel laminations and end plate) and has a magnetic length the same as the outer core. This produces an inner quarter core with the field free region which a magnetic length of 8.6 inches longer than the other inner quarter. The outer core length is 110.25 inches (2.8 meters) and the complete magnet has a flange to flange length of 128.375 inches. A 3 inch magnetic mirror plate is located between the end of the inner core assembly and the vacuum flange. The magnet is powered by a 24-turn single saddle coil. A nominal current of 2000 Amp. produces the required integrated field of 3.0 T-m. Figure 1 shows a cross section and longitudinal end view.

The magnetic requirements of a Lambertson septa for use in the Main Injector project have been presented elsewhere. [3] The first three requirements pertain to the bending field and effects either the extracted or injected beam.

\* Present address: AT&T Corp., Middletown, NJ.

† Operated by the Universities Research Association under contract with the U. S. Department of Energy

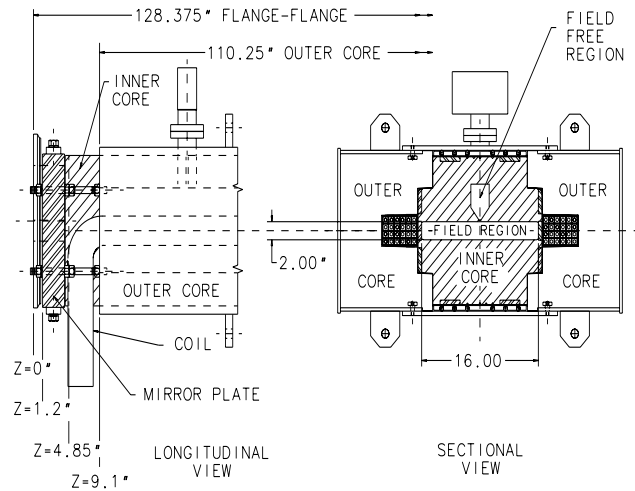


Figure 1: Geometry of the Lambertson

The last three requirements impact the behavior of the circulating beam in both the Tevatron and Main Injector. The final specifications used to build the production magnet are listed in Table 1.

TABLE 1: Magnetic Specifications

Nominal field	1.072	Tesla
Good field height	$\pm 6$	inches
Field Uniformity	$< 0.28$	percent
Leakage Field	$< 0.0114$	T-m
Leakage Gradient	$< .1$	Tesla-m/m
Leakage Sextupole	$< 9$	Tesla-m/m <sup>2</sup>

## 2 MAGNETIC MODEL

### 2.1 Two Dimensional Model

Magnetic 2-D modeling, with OPERA 2-D [1] was used to determine the detailed geometry of the Lambertson (i.e. the opening angle and radius of curvature of the field free region septum, the septum thickness, the pole tip shim in the dipole region, the height of the dipole region, and the placement of the stainless steel skin and tie bars) to minimize the leakage of the field from the steel into the field free region and maintain a high uniformity in the field region.

### 2.2 Three Dimensional Model

Early in the design of the end geometry of the Lambertson a 3D finite element code, TOSCA [1], was used to guide the end extension/mirror plate design. [5] A three foot prototype Lambertsons was constructed to test the magnetic design. The model was able to successfully predict the results of magnetic measurements from various end configu-

rations of the prototype and allow a better understanding of the the saturation effects in the end plate.

Subsequently, the 3D finite element model was updated to reflect the exact geometry of the production Lambertson including a realistic description of the permeability of the steel components. This model was used to calculate the dipole field (and its integral) through the end of the magnet for comparison with measured data.

### 3 MAGNET MEASUREMENTS

The Lambertson was oriented on the test stand at the Magnet Test Facility in orientation shown in Figure 1 such that a positive current produced a positive  $B_y$ . The coordinate system was defined such that  $x,y=0$  is in the center of the bend region and  $z=0$  is at the face of the vacuum flange (positive  $z$  is inside the magnet). Various measurement techniques were used to measure the fields in both the bending and field free region to confirm the design and compare with the 2-D and 3-D models.

### 4 FIELD REGION MEASUREMENTS

The field in the bending region was characterized using several methods to measure the integrated field, the field uniformity, and longitudinal extent of the dipole field over a 0 to 2500 A range. The dipole field in the bend region showed a 10 % falloff over the last 2 inches of the outer core and was down by a factor of 100 at the outside face of the mirror plate.

#### 4.1 Strength and Hysteresis

The excitation curve for the Lambertson was measured to 2500 A after a set of hysteresis ramps to the same maximum current. The field is quite linear up to 1500 A which corresponds to an integrated field of 2.4 T-m. The design integrated field of 3.0 T-m is achieved at 2000 A and deviates from the linear by roughly 6%. The maximum integrated field measured was 3.5 T-m at 2500 A. The integrated remnant field after the 2500 A hysteresis ramp is 42 Gauss-meter.

#### 4.2 Field Uniformity

The field uniformity along the  $x$  direction in the bending region was measured over  $\pm 7$  inches at  $y = 0$  and 0.5 inches using a 2-Wire Stretched Wire (2WSW) system which has a wire loop, separated by precision quartz rods at each end, stretched within the magnet aperture. Since the width of the wire loop is constant, the change in flux as the loop moves across the magnet aperture measures the variation in field strength as a function of position (field uniformity). The field at  $y = 0$  inches (not shown) is uniform to within 0.05% over the full  $\pm 7$  inches for all currents up to 2500A. Figure 2 shows the measured uniformity over the region from  $x=0$  to +8 inches for  $y=0.5$  inches, since it is symmetric in  $x$ . Here the field is uniform to within 0.1% out to  $\pm 6$  inches for all currents up to 2500 A, well within the specification. These measurements include both body and end

contribution to the integral. The predictions from the 2-D model include *only* the body field at 2000 A.

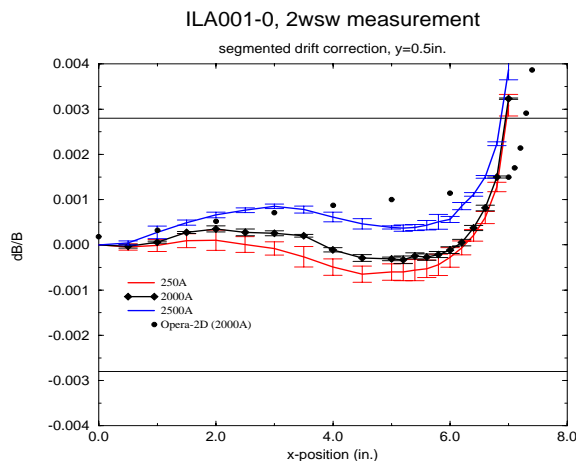


Figure 2: Comparison of the measured and 2D model field uniformity in the bend region at  $y=0.5$  inches.

### 5 FIELD FREE REGION

The fields in the field free region impact the circulating beam and therefore must be controlled. Contributions from both the body and the ends *must* be taken into account. By minimizing the integrated dipole, other harmonic terms will be minimized as well.

#### 5.1 End Field Shape

The magnitude of the dipole field on axis ( $x=0$ ) at approximately .35" from the septum was measured with a hall probe as a function of longitudinal position  $z$ . The probe consists of a Hall element and readout device which was operated under computer control. The readout device was programmed to read field values in Tesla using a full range of 3 Tesla. These probes have a precision of  $\pm 0.006\%$  of full range, and a resolution of  $\pm 0.5$  gauss on the 3 Tesla range. Positioning the probe was accomplished through the use of  $x$  and  $y$  stages. Probe motion was automated in the  $z$  direction.

The dipole field was measured using the hall probe at 1/2 inch intervals from a value of  $z = -8$  inches outside the end of the vacuum flange to  $z = +14$  inches, about 5 inches inside the body of the magnet. Measurements were taken at various excitations bracketing the expected operating range. Figure 3 displays the measured end field shape at 500 A, compares the measured end field shape with the prediction of the 3D model at 2000 A, and shows the integration of the 2000 A data from -8 inches to +9.1 inches. The effect of the mirror plate can be seen in the region between 4.35 and 4.85 inches, the gap between the end of the field free inner core and the steel mirror plate. Instead of jumping to the opposite pole, the leakage flux is channeled into the mirror plate around the field free hole and returned to the opposite pole. In this 1/2 inch region, the field has a transverse component (as seen by the large negative and positive fields

at the two surfaces, but the integrated effect cancels due to symmetry. Provided the plate remains out of saturation, the plate surface remains at a constant magnetic potential, and there should be no field outside the plate.

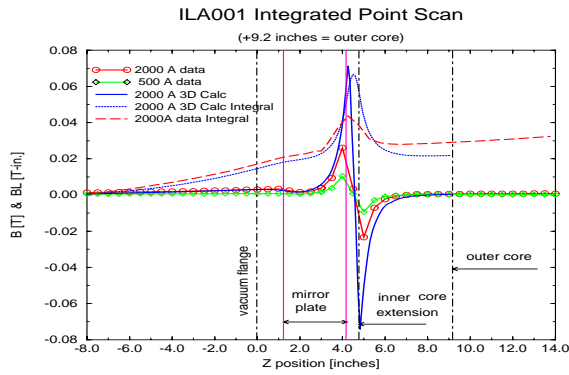


Figure 3: Comparison between the measured end dipole field and the predictions of the 3-D magnetic model as a function of  $z$  in the field free region at  $x=0, y=1.5$ . The  $z$  dimensions may be referenced to the orientation in figure 1.

### 5.2 Integrated Dipole

The integrated dipole in the field free region of the first production magnet was measured using several techniques. Figure 4 shows a comparison between the measured dipole field integral as a function of current for the various measurements and the predictions of the end field from the 3-D model. The first set of data shows the results of integrating the point scan data (in figure 3) through the magnet. The contribution to the total integral ( $2 \cdot \text{end} + \text{body}$ ) from the body and the end are displayed. The agreement between the measured end contribution (boxes) and the predictions from the 3D model is quite good with values between 5 and 7 G-m at 2000A. Both show a linear dependence. Uncompensated, the contribution to the dipole field integral from the magnet end surpassed 300 G-m.[5] Note that the major contribution to the total integral at the higher currents comes from the body field leakage and not the end field.

The next two sets of data were measured using a single stretched wire at the approximate the same location at point scan data. The Single Stretched Wire (SSW) system consists of moving a single wire stretched through the magnet aperture using high precision x-y stages while measuring the integrated voltage induced in the wire (flux). The return wire which completes the 'loop' is held fixed external to the magnet. Since the magnetic vector potential depends only on the wire position within the magnet, the change in flux through the loop only depends on the motion of the wire. The distance the stages move are measured to 1 micron accuracy by linear encoders, and so the absolute accuracy of the measured integrated field strength is a few times 10-4. This system was used to map the integrated field due to both the body and ends as a function of  $x$  and  $y$  inside the notch. The difference between the two data sets, taken on

two different days, reflect a systematic uncertainty in the measured value. The third set of data was obtained by integrating the dipole field using a rotating coil over each half of the magnet and summing the result. This data shows the effect of the hysteresis on the leakage between the up and down ramp. The up ramp data agrees well with the point scan data (taken at increasing currents).

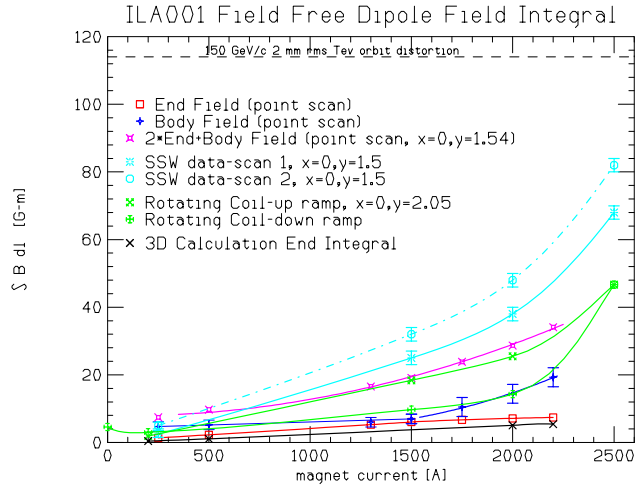


Figure 4: Comparisons between various measurements of the integrated dipole (at  $x=0, y=1.5$  inches) and the prediction of the 3-D model.

### 5.3 Harmonic Analysis

The harmonic content in the field free region was measured on axis,  $x=0$ , at three different values of  $y$  using a rotating coil. These measurements were done using a tangential coil probe with coil radii of 0.01219 meters and a length of 2.286 meters. This probe uses a dipole Morgan coil to measure the dipole integrated strength. Higher order harmonic components were obtained by monitoring the signal from a dipole bucked tangential coil. [4] The induced voltage in the coil was integrated for all coil configurations by a precision digital integrator. Data were captured over two complete probe rotations at 256 readings/rotation. The results to the rotating coil measurements showed the integrated harmonics for normal and skew quad and sextupole were well within the required specifications.

## 6 REFERENCES

- [1] Vector Fields, Oxford, England.
- [2] The Fermilab Main Injector Technical Design Handbook, August 1994.
- [3] D.E. Johnson, et.al. "Design of the Fermilab Main Injector Lambertson", proceedings 1995 PAC.
- [4] Henry D. Glass, "measurements of Harmonic Amplitudes and Phases Using Rotating Coils", MTF Note MTF-94-0004, 1994.
- [5] J.-F. Ostiguy and D.E. Johnson, "3D End Effects in Iron Septum Magnets", proceedings 1995 PAC.